

Effects of temperature on diblock copolymer micelle composed of poly(γ -benzyl L-glutamate) and poly(*N*-isopropylacrylamide)

Jae-Bok Cheon^a, Young-II Jeong^a, Chong-Su Cho^{*·b}

^aDepartment of Polymer Engineering, Laboratory of Biomedical Polymers, Chonnam National University, 300 Yongbong-dong, Kwangju 500-757, South Korea

^bCollege of Agriculture and Life Sciences, Seoul National University, 103 Serun-dong, Suwon 441-744, South Korea

Received 11 August 1997; accepted 22 May 1998

Abstract

Diblock copolymers composed of poly(γ -benzyl L-glutamate) and poly(*N*-isopropylacrylamide) (PNIPAAm) (abbreviated as GN) were prepared by the ring-opening polymerization of γ -benzyl L-glutamate *N*-carboxy anhydride (BLG-NCA) using amine-terminated PNIPAAm as a polymeric initiator. Polymeric micelles consisting of PBLG as the hydrophobic inner core and PNIPAAm as the hydrophilic outer shell were prepared by diafiltration method. Their critical micelle concentrations (cmc) were determined by fluorescent probe techniques with pyrene as a hydrophobic probe. The cmc of the polymeric micelle with the thermosensitive outer shell is less influenced by temperature than the ordinary polymeric micelle consisting of PBLG as the same innercore and poly(ethylene oxide) (PEO) as the hydrophilic outer shell (abbreviated as GE). Fluorescence results were used to estimate the thermodynamic data of micelle formation, such as the standard Gibbs energies (ΔG^0), the standard enthalpies (ΔH^0), and the standard entropies (ΔS^0) of micellization. For the GN/water system, ΔS^0 was found to be positive and so was favorable to micelle formation whereas ΔG^0 , ΔH^0 , and ΔS^0 for the GE/water system were found to be negative. The partition constant of pyrene in these micelles has a value of the order of 5 and inflection of the change of that for GN with temperature was found around the LCST of PNIPAAm. © 1999 Elsevier Science Ltd. All rights reserved.

Keywords: Critical micelle concentration (cmc); Fluorescence; Thermosensitive

1. Introduction

Amphiphilic block copolymers in various selective solvents can self-assemble to form aggregates on micellar structure with a solvophobic innercore and a solvophilic outershell. This phenomenon occurs above a critical concentration of the block copolymer, well known as the critical micelle concentration (cmc). For this reason, the self-assembly of amphiphilic molecules has received much attention, both experimentally [1–4] and theoretically [5–8], and has been groped for application such as catalysis [9], and drug delivery systems [10,11], etc. For such applications, information of the micellar properties such as the cmc, the size, the aggregation number, the stability, and the shape is needed first. The block lengths and compositions of each of the segments affect these properties [12,13]. As the solvophobicity of the solvophobic part of block copolymers increases, the cmc of block copolymers decreases, and the average aggregation number and size of the micelle

is increased since the solvent repulsion force of the solvophobic block and the interfacial tension between the solvent and the surface of the micellar core increase [12,13]. The size of solvent compatible block exerts an influence upon the micellar properties. These trends can be described and have been studied by conformational statics [7,11,14] and thermodynamics [15,16]. The theories by Nagarajan and Ganesh [13] and by Whitmore and Noolandi [12] suggest scaling relations for these micellar parameters which are proportional to $N_A^\alpha N_B^\beta$, where N_A is the length of the insoluble block and N_B the soluble block and α and β , the exponents of the scaling relation, represent the dependence of the micellar parameters on the block lengths. In the theory of Nagarajan and Ganesh [13], α and β for the *R* values were 0.73 and -0.17 for the polystyrene (PS) – polyisoprene in *n*-heptane and 0.7 and -0.08 for the PEO – poly(propylene oxide) (PPO) in water.

For block copolymers in organic solvents, micelle formation starts upon reducing the temperature and the enthalpy contribution is responsible for micellization [16–18]. The standard enthalpy of micellization of the copolymer become

* Corresponding author.

more negative when the length of the solvent-insoluble block is increased and the worse solvents for the core-forming block is used [19,20]. The standard entropy of micellization is negative and, therefore, unfavorable to the micellization process. In the case of the PEO-PPO-PEO/water system, an increase in temperature may cause remarkable micellization since PPO at above 15°C aggregates while the hydrophilicity of the PEO compared to PPO is nearly constant within the temperature range from 0–100°C.

There are a number of experimental methods available for the evaluation of cmc such as the surface tension, interfacial tension, light scattering, electrical conductivity, or osmotic pressure measurement as a function of concentration. One of the most powerful techniques for the determination of the cmc, the size, aggregation number is light scattering. However, scattering techniques are able to detect the onset of micellization only if the cmc occurs in a concentration region where this technique is sensitive and this experiment can be complicated by phenomena of secondary association [14]. Recently, fluorescence techniques have been suggested as a valuable tool for the investigation of many micellar properties [21–23]. This method can detect the onset of association for block copolymer at very low concentration on the order of 1 ppm [24]. Wilhelm et al. [25] developed the method for the cmc values for PS-*b*-PEO copolymers in water by the fluorescence study from pyrene (Py) which is well known as polarity-sensitive probe.

Poly(*N*-isopropylacrylamide) (PNIPAAm) is well known to exhibit a lower critical solution temperature (LCST) caused by the reversible formation and cleavage of the hydrogen bonding between the amide group and surrounding water molecules with temperature change in aqueous media. Ringsdorf et al. [26] reported thermally induced polymer conformational changes for the fluorescently labeled amphiphilic copolymers by fluorescently technique. Also, Taylor et al. [27] reported that the LCST was decreased with increasing hydrophobicity of the polymer.

In this study, the thermosensitive and ordinary block copolymers were prepared. The effect of the conformational change of the thermosensitive shell of the micelle composed of poly(γ -benzyl L-glutamate) (PBLG) and PNIPAAm on the micellization with temperature was investigated and compared to the ordinary polymeric micelle composed of PBLG and PEO. The fluorescent probe method for the cmc determination, proposed by Wilhelm et al. [25], was used. Thermodynamic data of the micelle formation was also estimated by the fluorescent method.

2. Experimental

2.1. Material

N-isopropylacrylamide (PNIPAAm) was obtained from Tokyo Kasei and purified by recrystallization in hexane. γ -benzyl L-glutamate *N*-carboxyanhydride (BLG-NCA)

was prepared according to the method described by Goodman et al. [28]. Mono amine-terminated PEO (MW = 12,000) was kindly supplied by Nippon Oil and Fat Co. and used without further purification. 2,2'-azobisisobutyronitrile (AIBN) was purchased from Polyscience Inc. 2-aminoethanethiol hydrochloride (AET·HCl) and KOH·methanol (Potassium hydroxide volumetric standard, 1.003 N solution in methanol) were obtained from Aldrich Chemical Company Inc.

2.2. Polymer synthesis

Amine-terminated PNIPAAm (ATPNIPAAm) was obtained according to the method previously reported by our group [29]. Briefly, ATPNIPAAm was prepared by radical polymerization of *N*-isopropylacrylamide (50 mmol) in MeOH (20 ml) at 60°C for 22 h by using AIBN (0.5 mmol) and AET·HCl (1.0 mmol) as initiator and chain transfer agent, respectively. The reaction mixture was degassed by three cycles of freeze–pump–thaw process prior to polymerization. KOH·methanol (1.0 mmol) was added to remove HCl from AET·HCl. The polymers were obtained by precipitation in diethyl ether. ATPNIPAAm was analyzed by gel permeation chromatography (GPC) to determine Mn and Mw of ATPNIPAAm. The reaction scheme is shown in Fig. 1(a).

GN diblock copolymer was obtained according to the method previously reported [29]. Briefly, the GN was prepared by ring-opening polymerization of BLG-NCA initiated with ATPNIPAAm in DMSO at 25°C at the total concentration of BLG-NCA and ATPNIPAAm of 3 wt%. The polymer was recovered by precipitation in diethyl ether after 72 h when the IR absorptions at 1860 cm⁻¹ and 1785 cm⁻¹ correspond to the stretching vibrations of the two carbonyl groups (C⁵ = O and C² = O) of BLG-NCA had disappeared. The reaction scheme is shown in Fig. 1(b).

Synthesis of GE diblock copolymer was carried out with the similar method of the GN diblock copolymer. The reaction scheme is shown in Fig. 1(c).

2.3. ¹H NMR measurement

¹H NMR spectra of the copolymers were measured in solvent CDCl₃ to estimate the copolymer compositions and the molecular weight of PBLG blocks, using a JEOL FX 90 Q NMR spectrometer.

2.4. GPC measurement

The molecular weight and molecular weight distribution were characterized by elution time relative to polystyrene monodisperse standards from GPC apparatus (Waters Model 590 HPLC pump, Milford, USA). An Ultrastyrigel 500 Å column and a Waters 410 differential refractometric detector were used. The mobile phase was THF with a flow-rate of 1.5 ml min⁻¹.

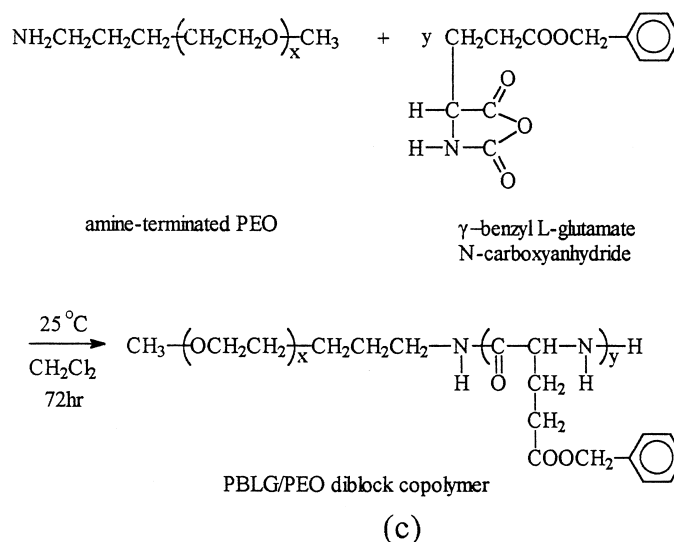
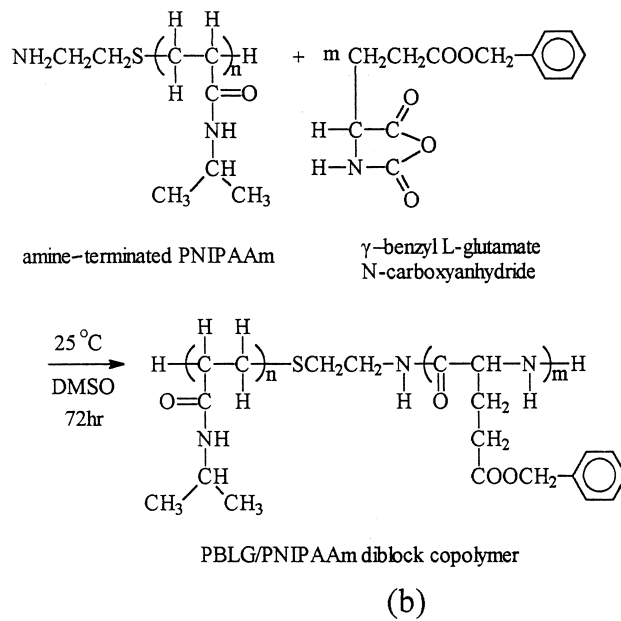
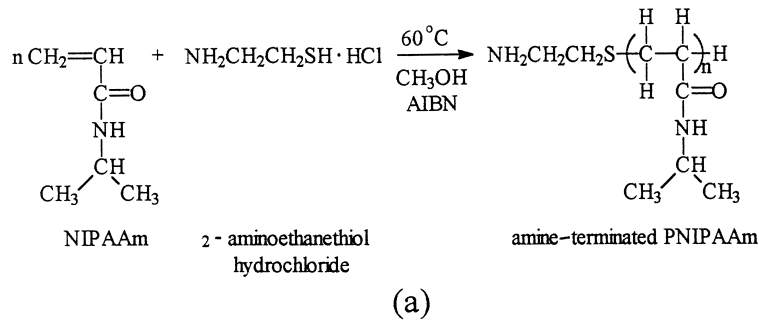


Fig. 1. Synthetic scheme for the preparation of (a) ATPNIPAAm, (b) PBLG/PNIPAAm block copolymer, and (c) PBLG/PEO block copolymer.

2.5. Preparation of stock solutions

Stock solutions were prepared by firstly dissolving the block copolymer (0.03 g) in the mixture of 10 ml of tetrahydrofuran/*N,N*-dimethylformamide[3/7 (v/v) for GN and

7/3 (v/v) for GEJ] in a 20-ml volumetric flask. The solutions were then dialyzed against distilled water using cellulose membrane tubing (12,000 molecular weight cutoff) for micellization and to remove the organic solvents for 48 h at room temperature. The distilled water was exchanged at

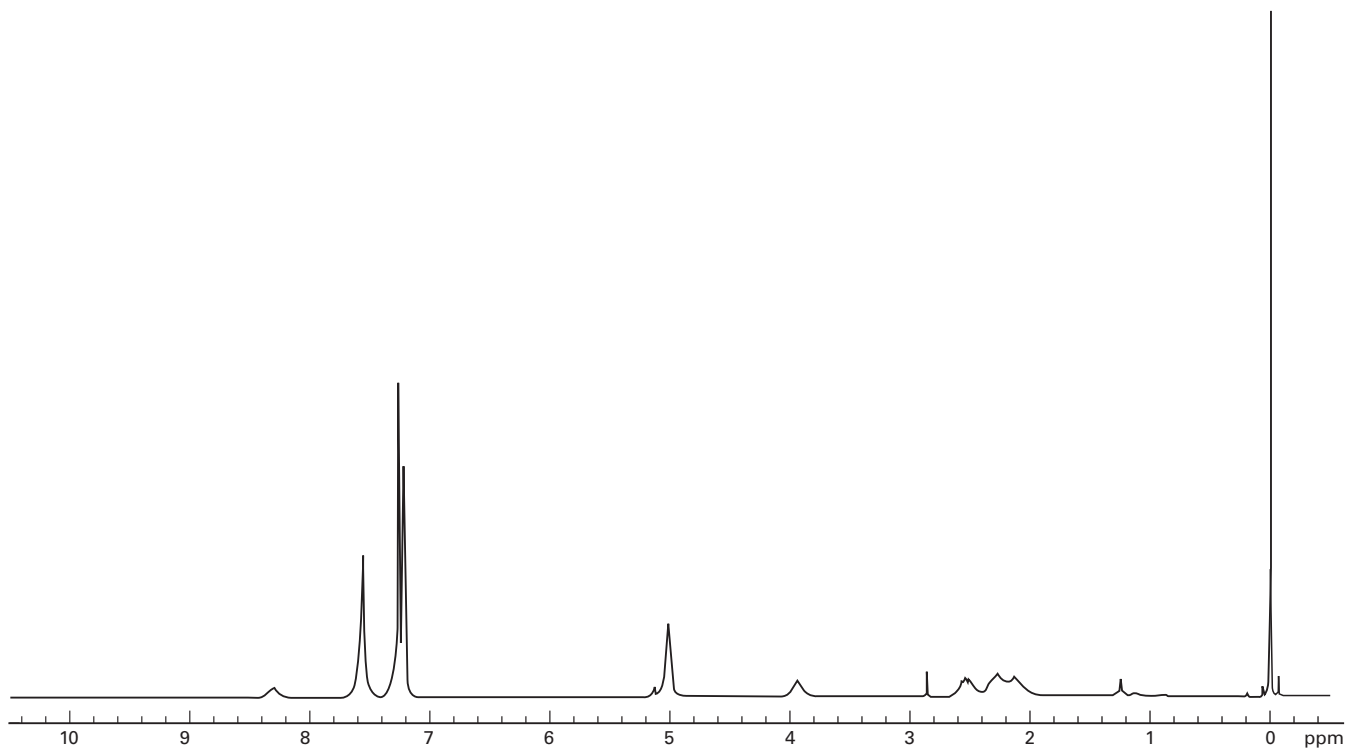


Fig. 2. Representative NMR spectrum for the GN-1 (a).

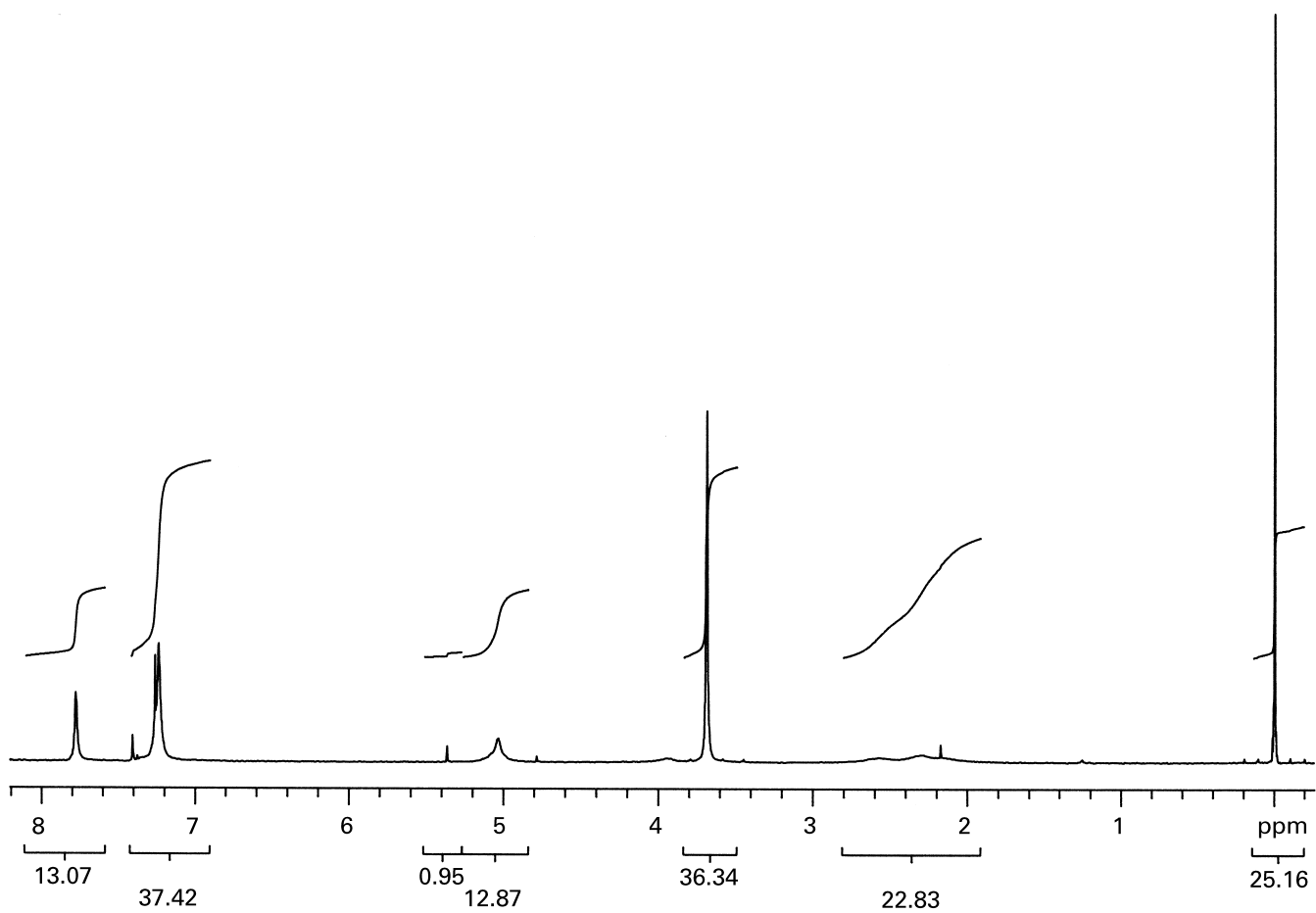


Fig. 2. Representative NMR spectrum for the GE-1 (b).

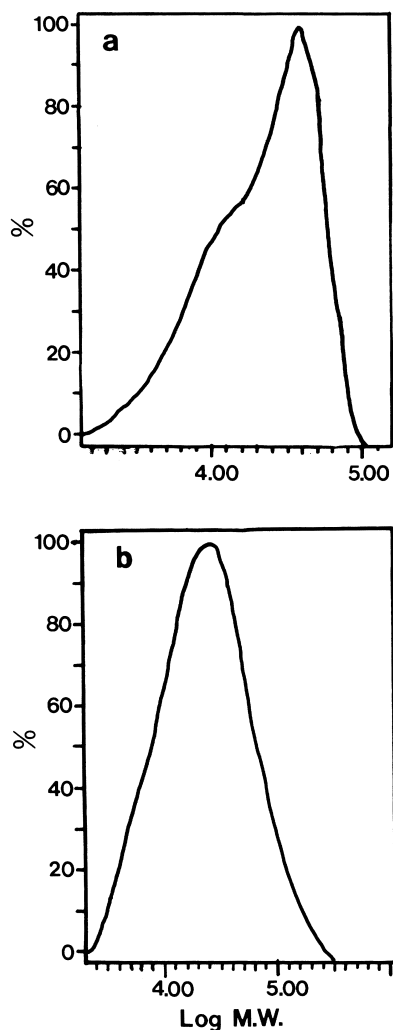


Fig. 3. Representative GPC spectrum for the GN-1 (a) and GE-1 (b).

intervals of 7–8 h. These solutions were diluted with water to 60 ml. Aliquots of the stock solutions were diluted with water to the desired concentration.

2.6. Sample preparation for fluorescence measurement

Sample solutions were prepared as follows: To each of 20.0 volumetric flasks a known amount of pyrene in acetone was added, chosen to give a Py concentration in the final solution of 6×10^{-7} M and the acetone was evaporated. To each flask was added a measured amount of a stock solution, followed by distilled water. The flasks were heated with stirring for 4 h at 60°C to an equilibrium of the pyrene and the micelles. The solutions were cooled and stirred overnight at room temperature. The samples ranged in polymer concentration from 1.0×10^{-4} – 0.5 g L^{-1} .

2.7. Dynamic light scattering (DLS)

The size of micelles were determined by photon correlation spectroscopy using an Malvern PCS 100 spectrometer

equipped with an Malvern 7032 correlator with the minimum sample time of 50 ns (system 4700, Malvern Instruments, UK). The argon ion laser beam at a wavelength of 488 nm and the scattering angle $\theta = 90^\circ$ were used. Micelle size distribution was measured at 25 and 34°C. The value is expressed in number-averaged scales as unimode. Before measurements, samples were filtered through a $0.45 \mu\text{m}$ filter. The typical micelle concentration used was 1 g L^{-1} .

2.8. Fluorescence measurements

Steady-state fluorescent spectra were measured using a JASCO FP-777 spectrofluorometer in the right-angle geometry (90° collecting optics) with a band width of 1.5 nm for excitation. All spectra were run on air-equilibrated solutions. For fluorescence excitation spectra, λ_{em} was 390 nm.

3. Results and discussion

GN and GE block copolymers were prepared by polymerization of BLG-NCA initiated by the amine-terminated PNIPAAm in DMSO and amine-terminated PEO in dichloromethane, respectively, as shown in Fig. 1(b) and (c). The representative NMR spectrum for the GN-1 and GE-1 is shown in Fig. 2(a) and (b), respectively. The GN block copolymer composition was estimated from the peak intensities of the signal of methylene protons (5.0 ppm) of the PBLG block and the signal of the methyne proton (4.2 ppm) of the isopropyl group in the PNIPAAm block in the spectrum. Also, the GE block copolymer composition was estimated from the peak intensities of the signal of methylene protons of the PBLG block and the signal of the ethylene proton (3.6 ppm) of the PEO block. The representative GPC spectra for the GN-1 (a) and GE-1 (b) are shown in Fig. 3. From the GPC results, the weight and number average molecular weights for the GN-1 are 38,238 and 32,656, respectively (polydispersity = 1.17). The weight and number average molecular weights for the GE-1 are 42,210 and 10,748, respectively (polydispersity = 3.93). It is not clear to have broad molecular weight distribution of GE-1 copolymer.

The compositions and molecular weights of the GN and GE block copolymers are shown in Table 1. In Table 2, the size of the micelles prepared by dialysis method were shown. The results of DLS for GN and GE micelles revealed that the size of the micelles ranged from 70–360 nm while polymeric micelles should be small and have the narrower size distribution. At this moment, the nature of the larger particle size is not clear. We consider several possibilities: (1) the individual micelles are further associated by the hydrophobic–hydrophobic interactions between exposed cores [30], (2) the multilayer structure with alternating concentric layers of solvated and undissolved blocks [14], and (3) secondary aggregate with time due to the weak steric stabilization of PNIPAAm and PEO chains [31]. Usually,

Table 1
Properties of PBLG/PNIPAAm (GN) and PBLG/PEO (GE) block copolymer in water

Sample	\bar{M}_n (PNIPAAm/PEO)	\bar{M}_n (PBLG)	χ_{PBLG}^a	cmc (g l ⁻¹)	10 ⁻⁵ K _f ^b
GN-1	23,000	8,500	0.27	0.0100	2.3
GN-2	23,000	15,200	0.40	0.0063	2.1
GN-3	23,000	27,000	0.54	0.0040	2.1
GE-1	12,000	8,400	0.41	0.0036	2.2
GE-2	12,000	39,800	0.77	–	–
GE-3	12,000	91,700	0.88	–	–

^aWeight fraction of PBLG.

^bEquilibrium constant for partitioning of pyrene between the aqueous and micellar phases.

the micelle sizes become larger as the content of PBLG increases, as expected. According to the study of Nagaragan et al. [13], micelles grow until the free energy per molecule of micellization reaches the minimum point with increasing aggregation number, mainly influenced by the free energy of formation of the micelle core-solvent interface. As the PBLG content becomes larger, the free energy per molecule of micellization has a minimum value at a larger aggregation number. As a consequence, the micellar size increases.

The changes of the photophysical and other properties of pyrene by virtue of its environment make it possible to study low and high molecular weight micelles [22,23,25], self-assembling monolayers [32,33], and membranelike systems of phospholipid dispersions [21,34], etc. They were focused on the fluorescence depolarization [22], shift of the (0,0) band in the excitation spectra, dynamics of quenching of pyrene monomer fluorescence [23], and excimer formation process [35,36]. The onset of intermolecular association of the amphiphilic block copolymers at the critical micelle concentration in water implies the formation of the hydrophobic environments. At this time, pyrene is preferentially solubilized into the inner part of these hydrophobic regions of the aggregates. Ultimately, the changes of the photophysical properties due to the transfer of pyrene from a polar environment to a nonpolar one give rise to the change of the three features of the excitation and emission spectra; a significant suppression in the intensity of the (0,0) vibronic band in comparison with other bands in the emission

spectra, an increase in the quantum yield of the fluorescence, a shift of the (0,0) band of the La(S_S ← S₀) transition from 334.5–339.5. By examining the extent of these changes as a function of block copolymer concentration, one can identify and determine the critical micelle concentration and equilibrium constant for the partitioning of the pyrene between the aqueous and the micelle core phases [25]. Astafieva et al. [37] attempted to apply the method of data treatment consisting of the deconvolution to the techniques of cmc determination suggested by Wilhelm et al. [25]. In accordance with one of the methods proposed by them, we estimated cmc through a red shift of the (0,0) band in the excitation spectrum of pyrene in water with increasing concentrations of block copolymer.

Fig. 4 presents a fluorescence excitation spectra obtained by measuring the fluorescence intensity ($\lambda_{\text{em}} = 390$) of a sufficiently dilute pyrene aqueous solution of GE-1 as a function of the exciting wavelength at various concentrations. An increase in the fluorescence intensity with increasing polymer concentration results from the enhancement of the lifetime of the excited state of the pyrene. It was found that the low-energy band of the La transition of pyrene shifted from 333–339 with increasing concentration of block copolymer as they was incorporated into the hydrophobic interior of the micelles. The dependence of the ratio I_{339}/I_{334} with the polymer concentration was shown in Fig. 5. The subscript of 339 and 333 were chosen as the wavelength of the (0,0) band at the lowest and highest polymer concentrations, respectively. In the concentration region below the

Table 2
Particle size distribution and association numbers of GN and GE series measured by dynamic light scattering and circular dichroism spectroscopy, respectively

Sample	PBLG (mol%)	Particle size (number average: nm)		Association numbers
		25°C	34°C	
GN-1	16.1	70 ± 12	110 ± 45	49.4
GN-2	25.6	350 ± 125	350 ± 250	–
GN-3	37.7	360 ± 180	300 ± 120	–
GE-1	12.4	200.5 ± 177	–	99.7
GE-2	40.0	251.9 ± 220.6	–	–
GE-3	60.5	309.9 ± 160.9	–	–

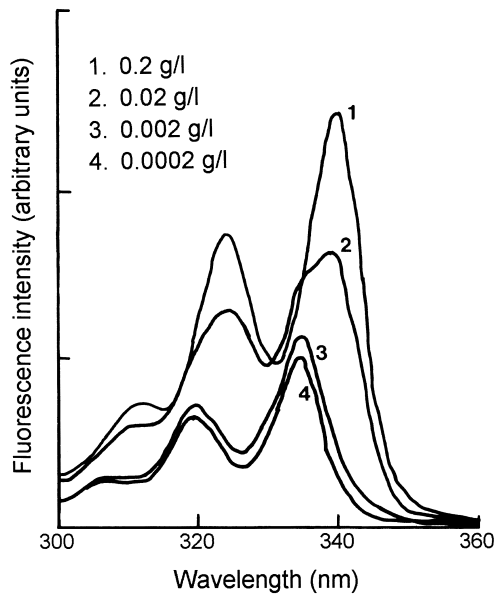


Fig. 4. Excitation spectra monitored at $\lambda_{em} = 390$ nm for the sample GE-1 showing the shift in the (0,0) band as pyrene partitions between aqueous and micellar environments.

cmc, the magnitude of I_{339}/I_{334} in Fig. 5 slightly increases because the amount of monomolecular micelles, which provide space for preferential binding of the pyrene molecules compared to the bulk water medium, is augmented with polymer concentration.

With increasing the block copolymer concentration in the rising part placed between the flat regions at low and high polymer concentrations, the micellization occurs and the micelle–unimer equilibrium moves towards the micelle continuously, which enhances the value of the I_{339}/I_{334} ratio, representing ultimately the extent of the pyrene solubilized into the micelle core.

When we determine the cmc, it may be expected that the

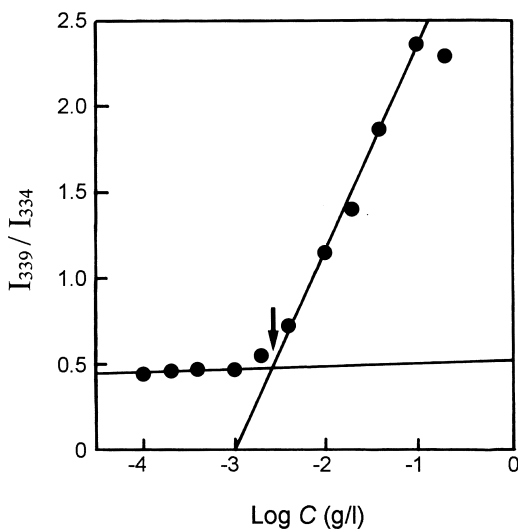


Fig. 5. Plots of the intensity ratios I_{339}/I_{334} from excitation spectra of the GE-1 block copolymer.

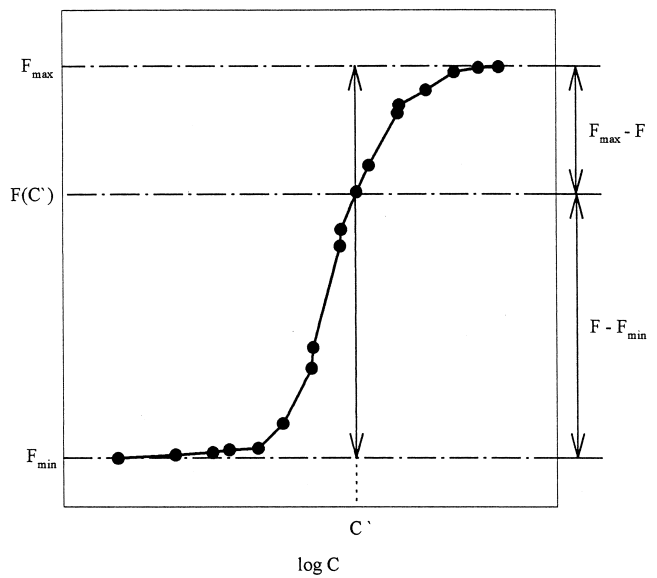


Fig. 6. Plots of $(F - F_{min})/(F_{max} - F)$ against $\log c$.

cmc exists in the inflection part between the flat region at the lowest polymer concentrations and the rising region in the sigmoidal curve as shown in Fig. 5. Then, how can it be taken? There are two methods for determination of the cmc from the excitation spectra.

The first is to take the intersection of two straight lines extendedly drawn through the points of the flat and drastically rising region of the plot. But, strictly speaking, it is not the concentration that shows the real onset of micellization in the block copolymers for the influence of the pyrene–unimer and the pyrene–micelle equilibria on the fluorescence data is not considered. For the determination of the true cmc, Wilhelm et al. [25] developed logically a new method, equivalent to the second, estimating whether the data fit better to a binding isotherm expressed in terms of cmc or in terms of the total concentration (c). And so the relationship equation as shown below has been obtained:

$$\frac{[Py]_m}{[Py]_w} = \frac{F - F_{min}}{F_{max} - F} = \frac{K_p \chi_A (c - cmc)}{1000 \rho_A} \quad (1)$$

where $F = I_{339.5}/I_{334.5}$, F_{min} and F_{max} correspond to the values of F on the straight line on the flat part at low and high polymer concentrations, respectively, as shown in Fig. 6. K_p is the equilibrium partition constant of the pyrene between a micellar phase and a water phase, c is the total polymer concentration ($g L^{-1}$), χ_A is the weight fraction of hydrophobic portion in the block copolymer, and ρ_A is the density of the micellar core, which in our system, is the density of the PBLG core of the micelle that was assumed to take the same values as that of PBLG with α -helical and crystal structure ($1.279 g ml^{-1}$) and we postulated that it does not change against temperature.

Plots of $(F - F_{min})/(F_{max} - F)$ vs. c shown in Fig. 6 enable one to obtain the true critical micelle concentration and plots of $(F_{max} - F)/(F - F_{min})$ vs. $1/(c - cmc)$,

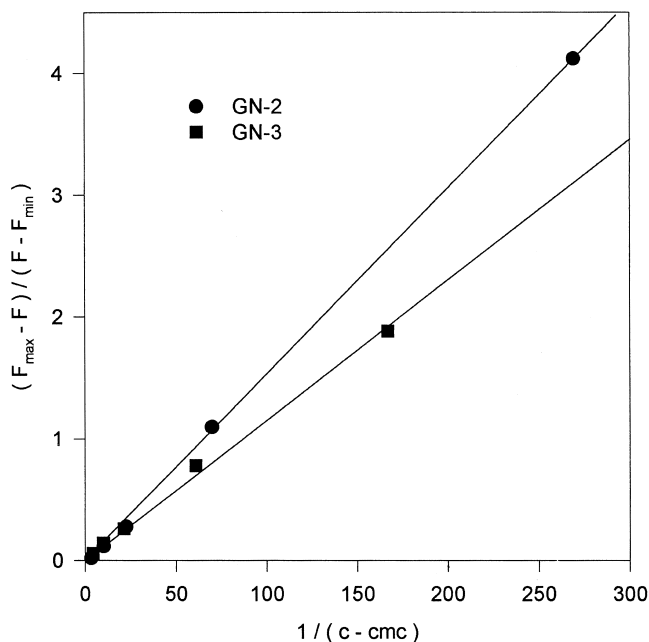


Fig. 7. Plots of $(F_{\max} - F)/(F - F_{\min})$ against $1/(c - \text{cmc})$ for GN-2 and GN-3 at 25°C.

which enable one to obtain the equilibrium partition constant [32]. Representative plots of $(F_{\max} - F)/(F - F_{\min})$ vs. $1/(c - \text{cmc})$ for GN-2 and GN-3 at 25°C are shown in Fig. 7.

Plots of the intensity ratio of $I_{339.5}/I_{334.5}$ (from pyrene excitation spectra) vs. $\log c$ for GN and GE block copolymers according to various temperature are shown in Figs 8 and 9, respectively. As the temperature increases, a shift of the cmc to the higher concentration is found due to the effect of temperature on the equilibrium between micelles and free chains. The equilibrium constant at low temperatures is relatively in favor of micelle formation compared to that at high temperatures. As shown in these figures, the increase of the cmc for GN is less than that for GE. This is originated from the enhancement of the micelle stability owing to the shrinkage of the outer shell, PNIPAAm, of the GN block copolymer. In the study on the dependence of the micellar properties on the size of the solvent compatible block done by Nagarajan and Ganesh [13], the shorter the length of the solvophilic block is, the lower the cmc becomes. Like this, as the hydrophilicity of the shell of GN-1 becomes lower against temperature, the cmc should come to be lower. However, the unimer–micelle equilibrium according to temperature counterbalances this effect. Consequently, the cmc slightly increases with temperature. The properties of the micelle such as cmc, aggregation number, and micellar size, etc., were largely affected by the length of the hydrophobic part of the block copolymer. In these experiments, because the molecular weight of the PBLG, hydrophobic part, of the GN-1 and GE-1 block copolymer is very similar to each other, the comparison of the change of the cmcs for these polymers is reasonable. We neglect the possibility of

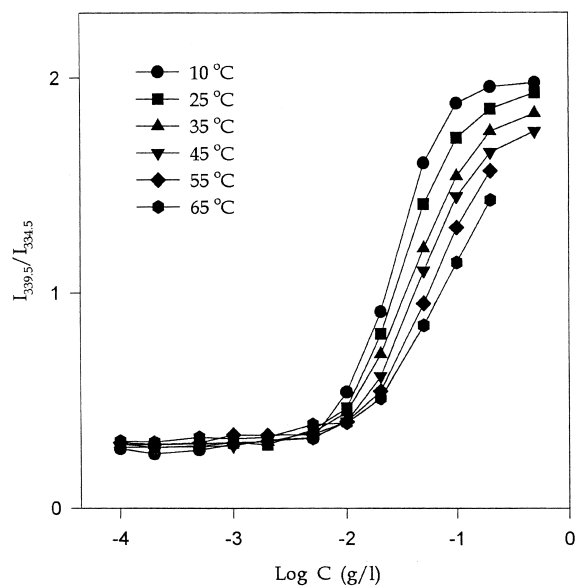


Fig. 8. Plots of the intensity ratio of $I_{339.5}/I_{334.5}$ (from pyrene excitation spectra) vs. $\log c$ for PBLG/PNIPAAm block copolymer (MW of PBLG: 8,500) according to various temperatures.

the solubilization of the pyrene to the shell in the GN polymer above the LCST of the PNIPAAm.

Plots of the cmc as a function of $1/T$ for solutions of GN and GE in water are shown in Fig. 10. All of these plots were linear within the experimental error over the dilute solution range studied. The slope corresponding to GN has a lower dependence on the temperature than that equivalent to GE as shown in Fig. 6.

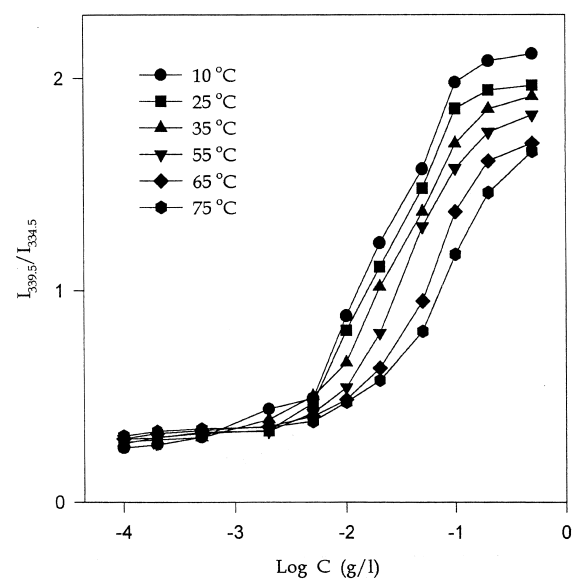


Fig. 9. Plots of the intensity ratio of $I_{339.5}/I_{334.5}$ (from pyrene excitation spectra) vs. $\log c$ for PBLG/PEO block copolymer (MW of PBLG: 8,400) according to various temperatures.

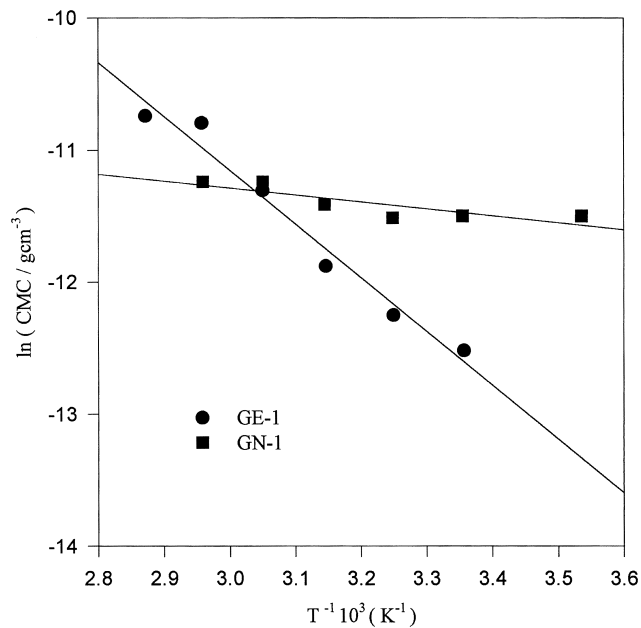


Fig. 10. Plots of cmc of GE-1 and GN-1 block copolymers against temperature.

Standard Gibbs energy, ΔG^0 , standard enthalpy, ΔH^0 , and standard entropy, ΔS^0 , of micellization were determined from the experimental data by means of the following equations:

$$\Delta G^0 \cong RT \ln(\text{cmc}), \quad (2)$$

$$\Delta H^0 \cong R \frac{d \ln(\text{cmc})}{dT^{-1}}, \quad (3)$$

$$\Delta S^0 \cong \frac{\Delta H^0 - \Delta G^0}{T}. \quad (4)$$

The thermodynamic data for micellization of the GN-1 and GE-1 copolymer in water at 25 and 65°C are given in Table 3. The standard Gibbs energies of micellization for both the GN and the GE copolymer are negative values, as expected. The negative standard enthalpy of micellization is caused by the exothermic interchange energy accompanying the replacement of PBLG segment/water interactions by PBLG segment/PBLG segment and water/water interactions in micelle formation. The enthalpy is responsible for micellization. In the GE/water system, the contribution of the negative standard entropy for micellization is nearly negligible. In the GN/water system, The standard entropy

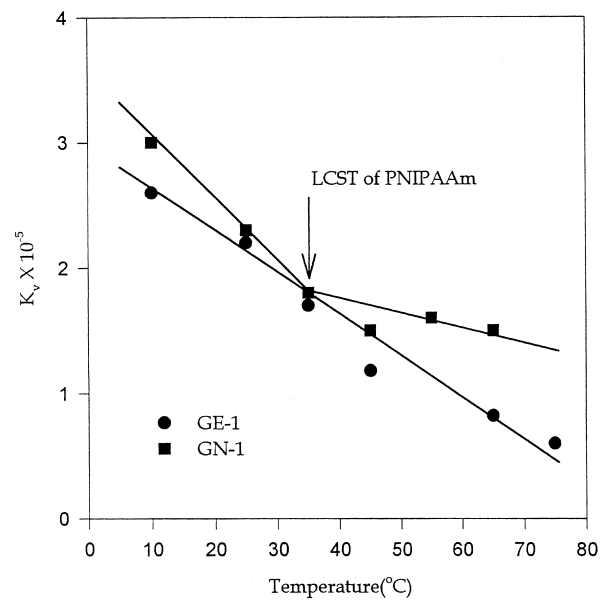


Fig. 11. Plots of the equilibrium constant (K_p) for partitioning of pyrene between the aqueous and micellar phases as a function of solution temperature for GN-1 and GE-1 in water.

shows a positive value and is responsible for micelle formation.

As shown in Fig. 11, the equilibrium constant for partitioning of pyrene between the aqueous and micellar phases for GE-1 decreases linearly within experimental error against temperature accompanying to the movement of the micelle–unimer equilibrium toward the micelle. But, in GN-1, the diminution rate of the equilibrium constant against temperature becomes less around the LCST of PNIPAAm because the conformational change of the PNIPAAm, as the shell of the micelle, protects the micelle having a hydrophobic core to solubilize the pyrene from the dissociation according to temperature.

4. Conclusion

Two sorts of micelles consisting of PBLG and PNIPAAm, or PEO were prepared and their micellar properties were characterized and compared to each other.

It was found that as the size of the hydrophobic part of block copolymers becomes larger, the size of the micelles is larger. GN micelle is more stable to the temperature than GE micelles due to the PNIPAAm in the diblock copolymer.

Table 3
Thermodynamic data for the micellization of the GN-1 and GE-3 block copolymer in water at 25 and 65°C

Sample	ΔG^0 (25°C) (kJ mol ⁻¹)	ΔG^0 (65°C) (kJ mol ⁻¹)	ΔH^0 (kJ mol ⁻¹)	ΔS^0 (kJ mol ⁻¹ K ⁻¹)
GN-1	- 28.5	- 31.6	- 4.37	0.0803
GE-3	- 31.1	- 30.4	- 33.9	- 0.009

The enthalpy factor in the GE/water system and both the entropy and enthalpy factors in the GN/water system are the driving force for micellization.

References

- [1] Xu R, Winnik MA, Riess G, Chu B, Croucher MD. *Macromolecules* 1992;25:644.
- [2] Desjardins A, Van de Ven TGM, Eisenberg A. *Macromolecules* 1992;25:2412.
- [3] Gao Z, Desjardins A, Eisenberg A. *Macromolecules* 1992;25:1300.
- [4] Zhong XF, Varsheny SK, Eisenberg A. *Macromolecules* 1992;25:7160.
- [5] Leibler L, Orland H, Wheeler JC. *J Chem Phys* 1983;79:3550.
- [6] Noolandi H, Hong KM. *Macromolecules* 1983;16:1443.
- [7] Halperin A. *Macromolecules* 1987;20:2943.
- [8] Birshtein TM, Zhulina EB. *Polymer* 1989;30:170.
- [9] Kitahara A. *Adv Colloid Interface Sci* 1980;12:109.
- [10] Kwon G, Suwa S, Yokohama M, Okano T, Sakurai KJ. *Contr Rel* 1994;29:17.
- [11] Rolland A, O'Mullane J, Goddard J, Brookman L, Petrek K. *J Appl Polym Sci* 1992;44:1195.
- [12] Whitmore MD, Noolandi J. *Macromolecules* 1985;18:657.
- [13] Nagarajan R, Ganesh K. *J Phys Chem* 1989;90:5843.
- [14] Xu R, Winnik MA, Hallet FR, Riess G, Croucher MD. *Macromolecules* 1991;24:87.
- [15] Teo HH, Yeates SG, Price C, Booth C. *J Chem Soc Faraday Trans* 1984;80:1787.
- [16] Bedells AD, Arafteh RM, Yang Z, Attwood D, Heatley F, Padget JC, Price C, Booth C. *J Chem Soc Faraday Trans* 1993;89(8):1235.
- [17] Price C, Kendall C, Stubbersfield RB, Wright B. *Polymer Commun* 1983;24:326.
- [18] Price C, Chan EKM, Mobbs RH, Stubbersfield RB. *Eur Polym J* 1985;21(4):355.
- [19] Quintana JR, Villacampa M, Muñoz M, Andrio A, Katime I. *Macromolecules* 1992;25:3125.
- [20] Price C, Chan EKM, Stubbersfield RB. *Eur Polym J* 1987;23:649.
- [21] Kalyanasundaram, K. *Photochemistry in microheterogeneous systems*. Orlando, FL: Academic Press, 1987.
- [22] Grieser F, Drummond CJ. *J Phys Chem* 1988;92:5580.
- [23] Almgren M, Lofroth JE, Van Stam J. *J Phys Chem* 1986;90:4431.
- [24] Zhao CL, Winnik MA, Riess G, Croucher MD. *Langmuir* 1990;6:514.
- [25] Wilhelm M, Zhao CL, Wang Y, Xu R, Winnik MA. *Macromolecules* 1991;24:1033.
- [26] Ringsdorf H, Venzmer J, Winnik FM. *Macromolecules* 1991;24(7):1678.
- [27] Taylor LD, Cerankowski C. *J Polym Sci, Polym Chem Ed* 1975;13:2551.
- [28] Fuller WD, Verlander MS, Goodman M. *Biopolymers* 1976;15:869.
- [29] Cho CS, Cheon JB, Jeong YI, Kim IS, Kim SH, Akaike T. *Macromol Rapid Commun* 1997;18:361.
- [30] Gao Z, Eisenberg A. *Macromolecules* 1993;26:7353.
- [31] Chung JE, Yokoyama M, Suzuki K, Aoyagi T, Sakurai Y, Okano T. *Colloids Surf B: Biointerfaces* 1997;9:37.
- [32] Chen SH, Frank CW. *Langmuir* 1991;7:1719.
- [33] Caruso F, Grieser F, Murphy A, Thistlethwaite P, Urquhart R, Almgren M, Wistus E. *J Am Chem Soc* 1991;113:4838.
- [34] Bohoquez M, Patterson LK. *J Phys Chem* 1988;92:1835.
- [35] Cao T, Munk P, Ramireddy C, Tuzar Z, Webber SE. *Macromolecules* 1991;24:6300.
- [36] Kiserov D, Prochazka K, Ramireddy C, Tuzar X, Munk P, Webber SE. *Macromolecules* 1992;25:461.
- [37] Astafieva I, Zhong XF, Eisenberg A. *Macromolecules* 1993;26:7339.